Electro-optic effects induced by the built-in electric field in a {001}-cut silicon crystal

Qi Wang (王 琦)[1], Zhang Hai (张 海)[1], Nian Liu (刘 念)[1], Baijun Zhao (赵佰军)[4], Xiuhuan Liu (刘秀环)[2,], Lixin Hou (侯丽新)[3], Yanjun Gao (高延军)[1], Gang Jia (贾 刚)[1], and Zhanguo Chen (陈占国)[1,*]**

[1]*State Key Laboratory on Integrated Optoelectronics, College of Electronic Science and Engineering, Jilin University, Changchun 130012, China*

[2]*College of Communication Engineering, Jilin University, Changchun 130012, China*

[3]*College of Information Technology, Jilin Agricultural University, Changchun 130118, China*

[4]*Changchun Institute of Applied Chemistry, Chinese Academy of Sciences, Changchun 130022, China*

**Corresponding author: czg@jlu.edu.cn; **corresponding author: xhliu@jlu.edu.cn*

Received July 6, 2015; accepted November 6, 2015; posted online December 16, 2015

Pockel's effect and optical rectification induced by the built-in electric field in the space charge region of a silicon surface layer are demonstrated in a {001}-cut high-resistance silicon crystal. The half-wave voltage is about 203 V, deduced by Pockel's effect. The ratio $\chi^{(2)}_{zxx}/\chi^{(2)}_{zzz}$ is calculated to be about 0.942 according to optical rectification. Our comparison with the Kerr signal shows that Pockel's signal is much stronger. This indicates that these effects are so considerable that they should be taken into account when designing silicon-based photonic devices.

OCIS codes: 230.2090, 190.4350.
doi: 10.3788/COL201614.012301.

Thanks to the expectations and efforts for all-silicon monolithic integration, silicon photonics has attracted a great deal of interest in recent years[1–4]. Among the various components of all-silicon monolithic integrated circuits[5–10], the optical modulator is a primary member[11,12]. It is well known that second-order nonlinear optical effects are absent in an ideal silicon crystal because of the property of center symmetry, which greatly limits the applications of silicon crystal in the optical modulator field.

Most of the current silicon modulators take advantage of the free-carrier plasma dispersion effect[13–16]. The bandwidth of these devices is always subject to the carrier lifetime and RC time constant which is the product of the resistance and capacitance, and these devices often have high light loss and power dissipation.

Pockel's effect (PE), also called the linear electro-optical effect, is not affected by the carrier lifetime, and it is possible to give it a large modulation bandwidth, owning to its extremely short response time with picosecond orders. Meanwhile, a small modulating voltage can be used for a dramatic phase and amplitude modulation[17]. In fact, an actual silicon crystal, an electric field or a magnetic field, or stress is able to break its inversion symmetry, which gives rise to an induced PE in the silicon crystal. Therefore, research on silicon modulators based on PE becomes a promising approach. The report of the strained silicon waveguide Mach–Zehnder interferometer modulator in 2006 gave us a boost in confidence, although the device has a small $\chi^{(2)}$ of 15 pm/V [18].

Near the silicon crystal surface, the existence of the built-in electric field in the space charge region (SCR) breaks the inversion symmetry[19], which produces the so-called electric-field-induced (EFI) second-order nonlinear optical effects. Compared with the strain-induced PE in silicon, the EFI-PE has a more simplified process in that it does not need another material, such as SiO_2 or Si_3N_4, to be deposited on the silicon layer. Realizing modulation only with a single silicon material is in favor of actualizing the all-silicon monolithic integration.

In previous experiments, we demonstrated the EFI-PE and optical rectification (OR) in the SCR of a silicon (111) surface layer using a metal-insulator-semiconductor-insulator-metal structure[20–22]. In this Letter, we demonstrate the EFI-PE and OR in the SCR of a silicon {001} surface layer. The half-wave voltage $V\pi$ and the ratio of $\chi^{(2)}_{zxx}/\chi^{(2)}_{zzz}$ are calculated. In addition, the Kerr effect is examined in the silicon crystal. The Kerr signal turns out to be much smaller than the EFI-PE signal. The PE and OR are so considerable in silicon that they should be taken into account when designing silicon-based photonic devices, especially modulators.

The sample is a {001}-cut high-resistance silicon single-crystal wafer sandwiched between two metal electrodes, as shown in Fig. 1(a). The silicon sample is an un-doped n-type single crystal with a resistivity of more than 1000 Ω cm. The size of the crystal is 20 mm × 10 mm× 3 mm. All six surfaces of the rectangular block wafer are polished before the experiments. In order to eliminate the free carrier plasma dispersion effect, a thick enough (160 μm) polyester insulating layer fills in each gap between the crystal surface and the electrode, which keeps the carriers from injecting into the crystal from the metal electrodes. The {001} surface layers of silicon possess C_{4v} symmetry, which means that the {001} surface layers can

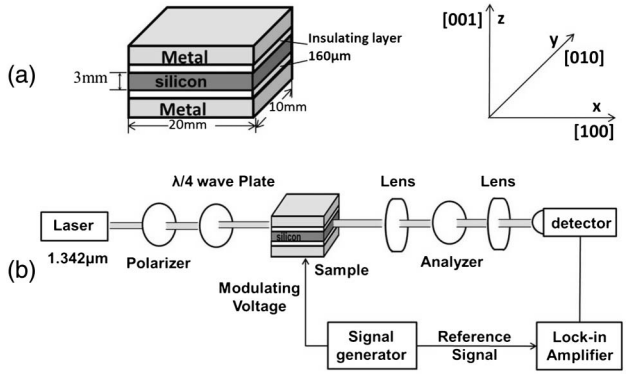

Fig. 1. Configuration of silicon sample and the measurement system for EFI PE. (a) MISIM configuration of silicon sample whose size is denoted. (b) Experimental measurement system for EFI PE.

be taken as uniaxial crystals whose optical axes are ⟨001⟩ axes[17]. According to the theory of PE[23], when a modulating electric field $\boldsymbol{E} = E_{0z}\cos(\Omega t)$ is applied along the [001] axis and the probing beam propagates along [010] direction, where Ω is the frequency of the modulating voltage, the phase retardation can be written as

$$\Delta\phi = \Delta\phi_0 + \Delta\phi(E), \tag{1}$$

where $\Delta\phi_0$ is the natural phase retardation because of the surface layer symmetry, and $\Delta\phi(E)$ is the phase retardation induced by the PE, and they are decided by

$$\Delta\phi_0 = \frac{2\pi}{\lambda}(n_e - n_o)l, \tag{2}$$

$$\Delta\phi(E) = 2\pi l\left(\frac{\chi^{(2)}_{zzz}}{n_e} - \frac{\chi^{(2)}_{xxz}}{n_0}\right)E_{0z}(\Omega)/\lambda, \tag{3}$$

where n_e and n_o are refractive indices of the extraordinary light and the ordinary light, respectively, l is the propagating length, λ is the wavelength of the probing beam in the vacuum, and $\chi^{(2)}_{zzz}$ and $\chi^{(2)}_{xxz}$ are the two non-zero components of the effective second-order susceptibility tensor.

The transverse electro-optic measurement system is shown in Fig. 1(b). A 10 kHz voltage is applied along the z-axis, and a light of 1342 nm from a 200 mW laser propagates through the SCR of the crystal surface layer along the y-axis. The total capacitance of the sample structure without a 10 kHz bias, about 31 pF, is measured. Most of the applied voltage drops on the insulating layer, and only a little voltage drops on the subsurface SCR of the silicon crystal, which satisfies the small signal model. The polarizations of the polarizer and the analyzer are 45° with respect to the x-axis on either side. The optical axis of the quarter-wave plate is parallel to the x-axis. Then, calculated by the Jones matrix, the intensity of the output beam I_o can be expressed as below:

$$I_o = I_i[1 \pm \sin(\Delta\phi)/2] \approx I_i[1 \pm \Delta\phi(E)/2], \tag{4}$$

where I_i is the intensity of the input beam. As for the case of the {001} surface layer SCR, $n_o \approx n_e$, so $\Delta\phi_0$ defined in Eq. (2) can be ignored. The output beam is somewhat dispersed when coming out from the silicon sample and the analyzer, so two lenses are used to focus the beam on a Ge photodetector.

The measured electro-optic signal curve is shown in Fig. 2. The electro-optic signal shows an almost perfectly linear relationship with the applied voltage, which is in agreement with the theoretical expectation.

The carrier density is about 4.46×10^{12} cm^{-3}, calculated according to the resistivity. So the Debye length L_D in the silicon surface layer can be calculated by

$$L_D = \sqrt{\varepsilon_0\varepsilon_{rs}kT/Ne^2}, \tag{5}$$

where ε_0 is the permittivity of free space, $\varepsilon_{rs} = 11.9$ is the dielectric constant of silicon, k is the Boltzmann constant, T is the absolute temperature in Kelvins, N is the carrier density, and e is the elementary charge. The result is $L_D \approx 1.96$ μm at 300 K. The flat-band capacity of silicon is estimated to be about 11.7 nF. The relationship between the measured electro-optical signal $V_{\rm eo}$ and the applied voltage $V_{\rm appl}$ is expressed as

$$V_{\rm eo} = \frac{1}{2}\alpha I_i \frac{\pi}{V_\pi}\frac{C_i}{C_i + C_s}V_{\rm appl}, \tag{6}$$

where $V_\pi = \lambda d/2(\frac{\chi^{(2)}_{zzz}}{n_e} - \frac{\chi^{(2)}_{xxz}}{n_o})l$ is the half-wave voltage, α is a factor depending on the photodetector and lock-in amplifier, d is the effective charge layer thickness, C_i is the capacity of the insulating layer, which is calculated to be about 33.2 pF, and C_s is the effective capacity of silicon crystal. In order to investigate the half-wave voltage V_π,

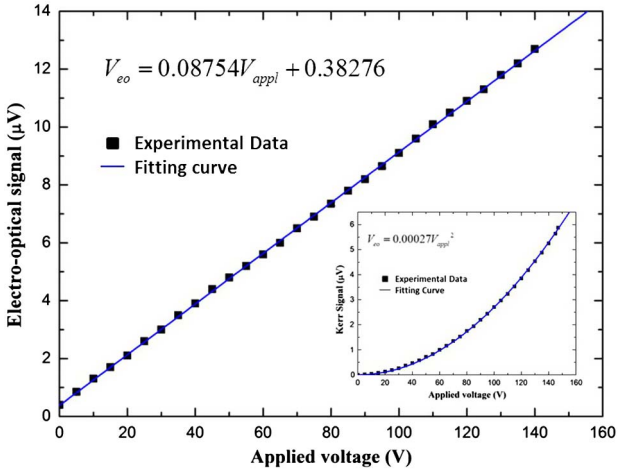

Fig. 2. Dependence of the electro-optic signal on the AC applied voltage for silicon sample with MISIM capacitor structure. The electro-optic response is linear with the applied voltage up to 140 V. The experimental curve is obtained without the external DC bias, so the linear electro-optic signal is induced by the built-in field in the SCR of the silicon sample. The insert figure is the measured Kerr signal.

we remove the silicon crystal and use a chopper instead of a signal generator to give the lock-in amplifier a reference signal. The optical signal is measure to be about 48.3 mV. However, the thickness of the SCR is only about 2.0 μm, and the light beam waist is more than 1 mm. So the light signal transmitting through the SCR is much less than 48.3 mV. Considering the slope of the fitted function in Fig. 2 and assuming $\frac{1}{2}\alpha I_i \approx 2$ mV, we estimate that the half-wave voltage V_π is about 203 V.

According to the theory of nonlinear optics, the Kerr effect becomes considerable in a centrosymmetric crystal. The measured electric-optic signal with the frequency of 2 Ω is the Kerr signal, which is shown in the insert figure of Fig. 2. The dependence of the Kerr signal on the applied voltage is a perfect quadratic curve. It is noted that the coefficient of the fitted function of Pockel's signal is over 300 times larger than that of Kerr signal. The ratio of the PE signal and the Kerr signal increases with the decrease of the applied voltage. At the applied voltage of 5 V, the EFI-PE signal is 41.5 times greater than the Kerr signal.

The OR can be taken as the inverse effect of the PE. Typically, they exist simultaneously in the SCR of silicon. In order to investigate the EFI-OR, the same silicon crystal that directly contacts the electrodes is used in the experiment, as shown in Fig. 3(a). The OR measurement system is shown in Fig. 3(b). The light propagates through the surface layer SCR of the silicon crystal along the y-axis. The polarization of the polarizer is parallel to the x-axis. Then, the dc polarization along the z-axis can be expressed as

$$P_z(0) = \varepsilon_0 |E(\omega)|^2 [(\chi^{(2)}_{zzz} + \chi^{(2)}_{zxx}) + (\chi^{(2)}_{zzz} - \chi^{(2)}_{zxx}) \cos(2\theta)], \tag{7}$$

where θ is the azimuth angle of the probing beam, $E(\omega)$ is the electric field strength of the probing beam, and $\chi^{(2)}_{zzz}$ and $\chi^{(2)}_{zxx}$ are the components of the effective second-order susceptibility tensor. By rotating the half-wave plate to change the azimuth θ, we measured the anisotropy of the EFI-OR, as shown in Fig. 4. It is clear that the OR signal

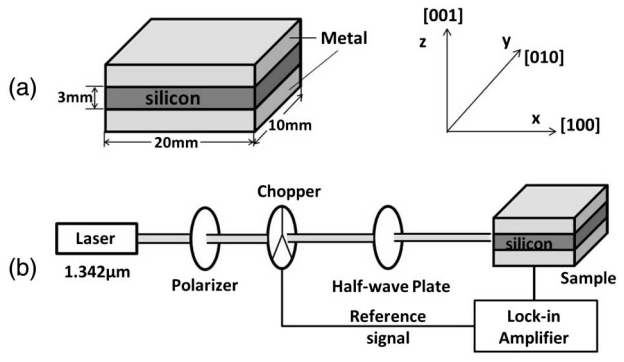

Fig. 3. Configuration of silicon sample and the measurement system for EFI OR. (a) MSM configuration of silicon sample. (b) The experimental system for measuring EFI OR. A half-wave plate is used to change the azimuth of the linearly polarized light.

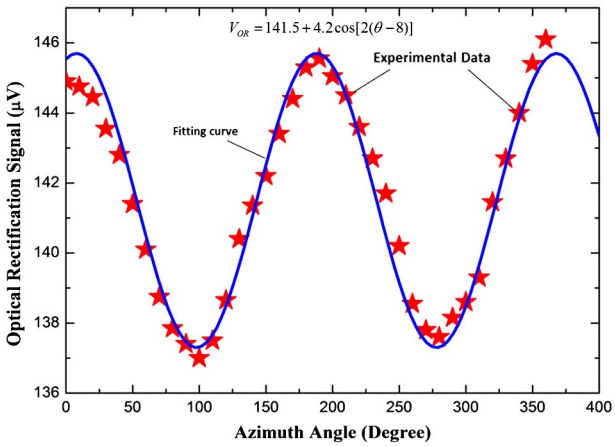

Fig. 4. Measured anisotropy of EFI OR in the SCR of the (001) surface layer of silicon crystal.

shows a cosine dependence on the azimuth θ. The solid line is the fitted curve, and the fitted equation is

$$V_{\mathrm{OR}} = 141.5 + 4.2\ \cos[2(\theta - 8)]. \tag{8}$$

The experimental result and fitted curve agree well with the theoretical formula [Eq. (7)]. It is noted that there is a considerable background independent of the azimuth θ, which corresponds to the first item on the right hand of Eqs. (7) and (8). One possible reason is that the values of $\chi^{(2)}_{zzz}$ and $\chi^{(2)}_{zxx}$ are very close, so their sum value is much larger than their difference value. Another contribution may be due to the absorption related to defects, impurities, and surface states, as our silicon crystal is merely n-type. Photo-generated carriers may be collected by the electrodes, giving rise to a detectable signal independent of the azimuth θ. If we neglect the latter factor and the influence of two-photon absorption, according to the fitted function of Eq. (6), the ratio of $\chi^{(2)}_{zxx}/\chi^{(2)}_{zzz}$ is calculated to be approximate to 0.942.

The EFI-PE is observed in the SCR of a {001}-cut un-doped n-type crystal. This conforms to our expectation because of the change of the symmetry in the SCR. The linear dependence of the PE signal on the applied voltage is perfect. Contrasted against the Kerr effect, the EFI-PE is much stronger. As always appears simultaneously with PE, the EFI-OR is also observed in the SCR of the sample. The experimental data and the fitted curve agree well with the theory. Using the corresponding relation between the coefficient of the experimental fitted curve and the theoretical formula, we estimate the ratio to be $\chi^{(2)}_{zxx}/\chi^{(2)}_{zzz} \approx 0.942$.

Our experiments manifest the EFI-PE and OR to be so conspicuous that these effects should be considered in designing silicon-based photonic devices, such as optical modulators and optical waveguides. In addition, these effects can be used as a tool to study the properties of the surfaces or interfaces of silicon devices.

This work was partially supported by the National Natural Science Foundation of China (Nos. 61474055 and 60976043) and the National 863 Program of China (No. 2009AA03Z419).

References

1. B. Jalali and S. Fathpour, J. Lightwave Technol. **24**, 4600 (2004).
2. R. Soref, IEEE J. Sel. Top. Quantum Electron. **12**, 1678 (2006).
3. Z. Zhou, B. Yin, Q. Deng, X. Li, and J. Cui, Photon. Res. **3**, B28 (2015).
4. M. Asghari and A. V. Krishnamoorthy, Nat. Photon. **5**, 268 (2011).
5. H. Rong, A. Liu, R. Jones, O. Cohen, D. Hak, R. Nicolaescu, A. Fang, and M. Paniccia, Nature **433**, 292 (2005).
6. J. Xing, Z. Li, P. Zhou, Y. Gong, Y. Yu, M. Tan, and J. Yu, Chin. Opt. Lett. **13**, 061301 (2015).
7. A. Liu, R. Jones, L. Liao, D. Samara-Rubio, D. Rubin, O. Cohen, R. Nicolaescu, and M. Paniccia, Nature **427**, 615 (2004).
8. Q. Xu, B. Schmidt, S. Pradhan, and M. Lipson, Nature **435**, 325 (2005).
9. C. Bao, Y. Yan, L. Zhang, Y. Yue, N. Ahmed, A. M. Agarwal, L. C. Kimerling, J. Michel, and A. E. Willner, J. Opt. Soc. Am. B **32**, 26 (2015).
10. N. Cartiglia, M. Baselga, G. Dellacasa, S. Ely, V. Fadeyev, Z. Galloway, S. Garbolino, F. Marchetto, S. Martoiu, G. Mazza, J. Ngo, M. Obertino, C. Parker, A. Rivetti, D. Shumacher, H. Sadrozinski, A. Seiden, and A. Zatserklyaniy, J. Instrum. **9**, C02001 (2014).
11. J. Wang, L. Zhou, H. Zhu, R. Yang, Y. Zhou, L. Liu, T. Wang, and J. Chen, Photon. Res. **3**, 58 (2015).
12. T. Li, D. Yang, and J. Wang, Chin. Opt. Lett. **12**, 082501 (2014).
13. L. Liao, A. Liu, D. Rubin, J. Basak, J. Basak, Y. Chetrit, H. Nguyen, R. Cohen, N. Izhaky, and M. Paniccia, Electron. Lett. **43**, 1196 (2007).
14. P. Dong, S. Liao, D. Feng, H. Liang, D. Zheng, R. Shafiiha, C.-C. Kung, W. Qian, G. Li, X. Zheng, A. V. Krishnamoorthy, and M. Asghari, Opt. Express **17**, 22484 (2009).
15. H. Xu, X. Xiao, X. Li, Y. Hu, Z. Li, T. Chu, Y. Yu, and J. Yu, Opt. Express **20**, 15093 (2012).
16. K. Ogawa, K. Goi, A. Oka, Y. Mashiko, T.-Y. Liow, X. Tu, G.-Q. Lo, D.-L. Kwong, S. T. Lim, M. J. Sun, and C. E. Png, Proc. SPIE **9367**, 93670C (2015).
17. A. Yariv and P. Yeh, *Optical Waves in Crystals* (John Wiley, 2003).
18. R. S. Jacobsen, K. N. Andersen, P. I. Borel, J. Fage-Pedersen, L. H. Frandsen, O. Hansen, M. Kristensen, A. V. Lavrinenko, G. Moulin, H. Ou, C. Peucheret, B. Zsigri, and A. Bjarklev, Nature **441**, 199 (2006).
19. J. E. Sipe, D. J. Moss, and H. M. van Driel, Phys. Rev. B **35**, 1129 (1987).
20. Z. Chen, J. Zhao, Y. Zhang, G. Jia, X. Liu, C. Ren, W. Wu, J. Sun, K. Cao, S. Wang, and B. Shi, Appl. Phys. Lett. **92**, 251111 (2008).
21. J. Zhu, Z. Chen, X. Liu, Y. Gao, J. Mu, Z. Wang, W. Han, and G. Jia, Opt. Laser Technol. **44**, 582 (2012).
22. J. Zhu, Z. Chen, X. Liu, J. Mu, Y. Gao, W. Han, and G. Jia, Chin. Opt. Lett. **10**, 082301 (2012).
23. A. Yariv, *Introduction to Optical Electronics* (Holt, Rinehart and Winston, 1976).